Electronic structure of the lead monoxides: Band-structure calculations and photoelectron spectra

H. J. Terpstra, R. A. de Groot, and C. Haas
Materials Science Center, Laboratory of Chemical Physics, University of Groningen, Nijenborgh 4, 9747 AG Groningen, The Netherlands
(Received 16 March 1995; revised manuscript received 18 May 1995)

PbO is a layer compound which exists in two polymorphic forms, a red tetragonal (α) and a yellow orthorhombic (β) modification. *Ab initio* band-structure calculations are presented for both phases. The calculated energy gaps are in agreement with optical data. The band-structure calculations are used to discuss the chemical bonding in the α and β phases. It is found that the Pb 6*s* states are strongly hybridized with O 2*p* orbitals. Thus the so-called Pb $(6s)^2$ lone pair in PbO takes part in the chemical bonding, and cannot be considered as an inert pair. Photoelectron spectra of the valence band and of some core levels are presented for α- and β-PbO. The observed valence band is in good agreement with the calculated band structure.

I. INTRODUCTION

Lead monoxide has long been known to occur in two polymorphic forms: a red, tetragonal α modification stable at room temperature[1] and a yellow, orthorhombic β form that is stable above 760 K.[2] These phases occur naturally as the minerals litharge and massicot, respectively. Both phases have a layered structure. These oxides are technologically important because they exhibit photoactivity over a wide range of wavelengths.[3–6] For this reason they are used in imaging devices, in television pickup tubes (Plumbicom),[3] electrophotography,[7] and electroradiography.[8]

Below 208 K, α-PbO transforms into a distorted, incommensurate α' phase.[9–14] The tetragonal α phase is stable at room temperature for pressures below 0.7 GPa; the orthorhombic β phase is stable for pressures above 2.5 GPa. In the intermediate region between 0.7 and 2.5 GPa, an orthorhombic γ phase was reported to be stable at room temperature.[15] This γ phase is an orthorhombic distortion of the tetragonal α phase, and it is formed from the α phase by a second-order phase transition.

Divalent lead compounds have an interesting structural chemistry.[16] In several compounds the heavy post-transition elements, especially thallium, lead, and bismuth, have an oxidation number two less than the group number. This is ascribed to the stability of a so-called inert pair of electrons.[16–18] The $6s^2$ pair of the free Pb^{2+} ion is stereochemically active: in many divalent lead compounds these electrons are not in a spherically symmetrical orbital, but stick out to one side of the Pb^{2+} ion, resulting in a distortion of the metal ion coordination.

In this paper we present studies of the electronic structure of PbO using *ab initio* band-structure calculations and photoelectron spectra. The chemical bonding in both phases of PbO is discussed. We compare our results with several semiempirical band-structure calculations that are available for PbO.[19–22] Very few experimental investigations on the electronic structure of lead oxides have been reported. There are some x-ray photoelectron spectroscopy (XPS) studies on lead oxides,[23–25] but these studies are restricted to a few core levels. To our knowledge, no experimental data on the valence-band structure are known.

II. CRYSTAL STRUCTURES

A. Crystal structure of α-PbO

The low-temperature phase of lead monoxide, which is thermodynamically stable at room temperature, is a tetragonal distortion of the CsCl structure with space group $P4/nmm\text{-}D_{4h}^7$ (No. 129), $Z=2$. The axes at 300 K are $a=0.3974$ nm and $c=0.5021$ nm.[9] The lead atoms occupy the 2*c* position with coordinates $(0,\frac{1}{2},u)$ and $(\frac{1}{2},0,\bar{u})$ with $u=0.237$. Oxygen atoms occupy the 2*a* position with coordinates (0,0,0) and $(\frac{1}{2},\frac{1}{2},0)$. Each lead atom is bound to four oxygen atoms forming a square pyramid with a lead atom at the apex, with Pb-O distances of 0.232 nm (see Fig. 1). The other four oxygen atoms are at 0.432 nm. Each oxygen atom is surrounded tetrahedrally by four lead atoms. As can be seen clearly from the figure, α-PbO has a layered structure, with the layers parallel to the *ab* plane. Within each layer, the ox-

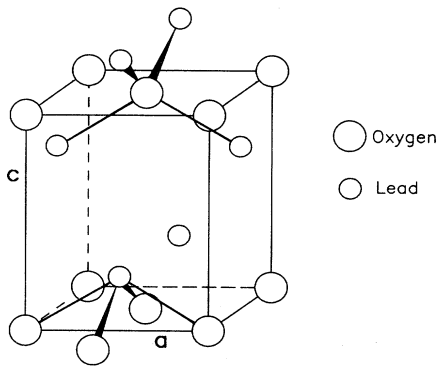

FIG. 1. Crystal structure of α-PbO.

0163-1829/95/52(16)/11690(8)/$06.00

ygen atoms are sandwiched between two lead sublayers. The distance between lead atoms of the two layers is 0.386 nm, which is 10% larger than the Pb-Pb distance of 0.350 nm in lead metal.

At 208 K there is a second-order phase transition from the α phase to an incommensurate structure, the so-called α' phase.[9] This $\alpha \rightarrow \alpha'$ transition is characterized by very small atomic displacements. There is a modulation vector along the [110] direction in reciprocal space that breaks the tetragonal symmetry and leads to an average orthorhombic symmetry with space group *Cmma* (No. 67), $Z=4$. The symmetry of the modulated phase is described by the four-dimensional superspace group $P(C2mb):(\bar{1}\,\bar{1}1)$,[10] or according to a recent study, $P(Cmma):(s\bar{1}1)$.[14] The high-pressure orthorhombic γ phase has a structure intermediate between the structures of the α and β phases.[15]

B. Crystal structure of β-PbO

Above 765 K the thermodynamically stable phase is β-PbO, but this phase is metastable at room temperature. β-PbO crystallizes in the orthorhombic system with space group $Pbcm$-D_{2h}^{11} (No. 57), $Z=4$; see Fig. 2.[2] The axes are $a=0.58931$, $b=0.54904$, and $c=0.47528$ nm (at 300 K). Both the lead and the oxygen atoms occupy the 4*d* position with coordinates $\pm(x,y,\frac{1}{4};\bar{x},y\pm\frac{1}{2},\frac{1}{4})$ with x(Pb)=0.2297, y(Pb)=0.9884, x(O)=0.8653 and y(O)=0.0917. Within a layer of orthorhombic β-PbO, two oxygen sublayers are sandwiched between two lead sublayers, which form the outside of the layers. The layers, which are parallel to the *bc* plane, are made up of parallel -Pb-O-Pb-O- zigzag chains. The lead atoms are in a distorted square-pyramidal coordination, with Pb-O distances of 0.2221, 0.2249 (within the chains), and 2×0.2481 nm (between the chains). The mean Pb-O distance is 0.2358 nm, which is somewhat larger than in α-PbO. The next-nearest oxygen atom is 0.3360 nm away. The oxygen atoms lie in the interior of the sheets in a distorted tetrahedral coordination. The distance between lead atoms of two layers is 0.3977 nm, so the distance between layers in β-PbO is larger than in the α phase.

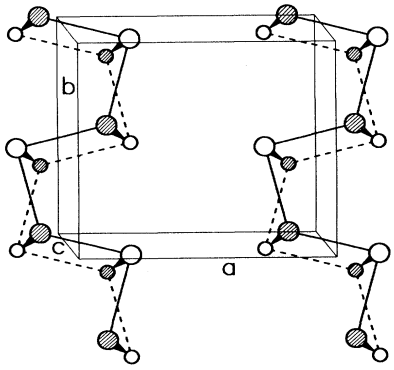

FIG. 2. Crystal structure of β-PbO. The open circles represent the lead atoms, the oxygen atoms are hatched. Large circles are at $z=0.25$, small circles are at $z=0.75$.

III. BAND-STRUCTURE CALCULATIONS

A. Details of the calculation

For the band-structure calculations the augmented spherical wave (ASW) method of Williams, Kübler, and Gelatt[26] was used. Exchange and correlation were treated within the local-spin-density approximation.[27] Scalar relativistic effects (mass velocity and Darwin terms) were included as described by Methfessel and Kübler.[28] To take into account the spin-orbit interaction, an extra term $\lambda\mathbf{L}\cdot\mathbf{S}$ was incorporated in the Hamiltonian. The value of the spin-orbit coupling parameter λ was obtained from Ref. 29. Self-consistency was achieved in about 20 iterations to a precision of $1:10^{-5}$.

The most important approximations of the ASW method are the use of a spherically symmetric potential within each Wigner-Seitz cell and the local-density approximation. The core electrons of a certain atom are confined to the corresponding Wigner-Seitz cell; i.e., effects due to direct kinetic transfer of core electrons between different cores are neglected.

The basis functions were composed of 6*s*, 6*p*, and 6*d* functions on the Pb sites and 2*s* and 2*p* functions on the O sites. Pb 5*f* functions and O 3*d* functions were included in the internal summation of the three center contributions to the matrix elements, which can be interpreted as treating these features as a perturbation. The choice of these basis functions implies that the small contribution of Pb 6*d* to the chemical bonding is taken into account. However, because the Pb 5*d* orbitals were treated as core states, the hybridization of Pb 5*d* with other orbitals is neglected in the calculations. As a consequence, it was not possible to obtain reliable results for the O 2*s* bands. The reason is that the orbital energies of O 2*s* and Pb 5*d* are about the same (binding energies of about 17 eV) and the Pb 5*d*–O 2*s* hybridization matrix elements are large. The neglect of the hybridization of Pb 5*d* states is expected to have only a small effect on the higher valence and conduction bands and on the chemical bonding.

Generally the band structures obtained with the ASW method depend on the values of the Wigner-Seitz radii. We have carried out ASW band-structure calculations for α- and β-PbO with various sets of Wigner-Seitz radii, ranging from R(Pb)=1.591 Å, R(O)=1.137 Å to R(Pb)=1.401 Å, R(O)=1.401 Å. It was found that the overall band structures change only slightly as a function of the Wigner-Seitz radii: the dispersion, the ordering, and the orbital character of the bands remain essentially the same. However, there are small energy shifts of the order of 0.2–0.5 eV. For example, the energy gap of α-PbO changes from 1.82 eV for R(Pb)=1.575 Å, R(O)=1.167 Å to 1.53 eV for R(Pb)=1.492 Å, R(O)=1.297 Å. The Wigner-Seitz radii used for the band structures reported in this paper were chosen in such a way that the overlap between the various Wigner-Seitz spheres was well balanced and not larger than 5 vol %. The ratio of these radii is the same as the ratio of the averages of the ionic and covalent radii of the atoms. When the crystal structure is not densely packed, as is certainly the case in the layered lead monoxides, it is

TABLE I. Input parameters for the band-structure calculation of α-PbO.

Atom	Start configuration	R_{WS} (Å)	Atomic position
Pb	$[Xe]4f^{14}5d^{10}6s^26p^2$	1.575	2c (z=0.237)
O	$[He]2s^22p^4$	1.167	2a
ES1	$1s^02p^0$	1.256	2b
ES2	$1s^02p^0$	1.256	2c (z=0.734)

necessary to include empty spheres (ES) in the calculation. For both α-PbO and β-PbO two types of empty spheres are included. The atomic positions and the Wigner-Seitz sphere radii (R_{WS}) used in the band-structure calculations are tabulated in Tables I and II.

B. Band structure of α-PbO

The first Brillouin zone of the α phase with the tetragonal primitive space group is also simple tetragonal and is shown in Fig. 3(a). The calculated energy bands are shown in Fig. 4. We have used the symmetry notations of Miller and Love.[30] The total and partial density of states are shown in Fig. 5.

The charges in the muffin-tin spheres and the orbital configuration of atoms and empty spheres are given in Table III. Not too much significance should be given to the charges, because they are strongly dependent on the Wigner-Seitz radii, and the presence of empty spheres. For example, if we use the same radii for the empty spheres and R_{WS}(Pb)=1.492 Å and R_{WS}(O)=1.297 Å we find Q(Pb)=+1.57 and Q(O)=−0.71, whereas the charges on the empty spheres remain almost the same.

The lowest-lying states of the valence band have mainly Pb 6s character (60%), but there is an appreciable amount of mixing with O 2p states (35%) (see Fig. 5). In large parts of the Brillouin zone, the lower two bands are separated from the rest of the valence band. The next four valence bands, between binding energies 2.1 and 4.7 eV (relative to the top the valence band), consist of O $2p_{x,y}$ states, hybridized with Pb $6p_{x,y}$ states. At the top of the valence band there are two bands with predominantly O 2p character, but with strong hybridization with Pb 6s states and Pb $6p_z$ states.

In Table IV we have listed the symmetry and wave function character of the valence-band states and the lowest conduction-band state at Γ. Only orbitals that contribute more than 10% to the eigenvalues are listed. The lowest- and highest-lying levels of the valence band are both of Γ_{3-} symmetry and have large contributions of O $2p_z$ and Pb 6s orbitals. The minimum of the con-

TABLE II. Input parameters for the band-structure calculation of β-PbO.

Atom	Start configuration	R_{WS} (Å)	Atomic position
Pb	$[Xe]4f^{14}5d^{10}6s^26p^2$	1.542	4d (x=0.2297, y=0.9884)
O	$[He]2s^22p^4$	1.131	4d (x=0.8653, y=0.0917)
ES1	$1s^02p^0$	1.395	4c (x=0.4865)
ES2	$1s^02p^0$	1.105	4c (x=0.0270)

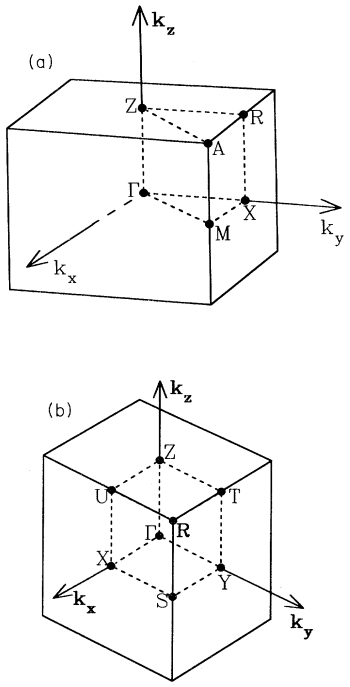

FIG. 3. First Brillouin zone of (a) α-PbO, (b) β-PbO.

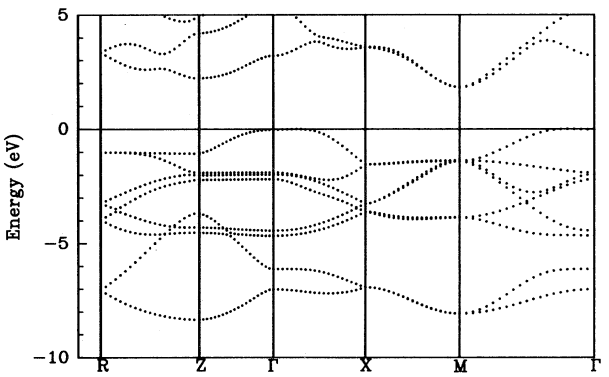

FIG. 4. The band structure of α-PbO; the energies are with respect to the top of the valence band.

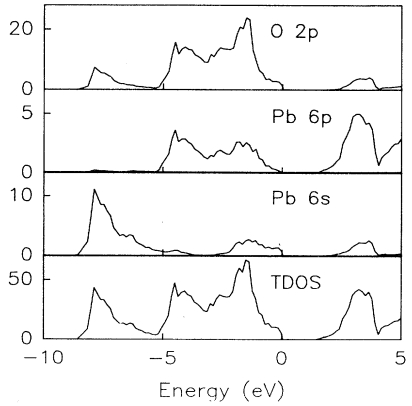

FIG. 5. Total and partial density of states for α-PbO.

TABLE III. Charges Q in the WS sphere and atomic configuration of atoms and empty spheres for α-PbO.

Atom	Q	Configuration
Pb	+1.19	$6s^{1.52}6p^{0.87}6d^{0.28}(5f^{0.14})$
O	−0.37	$2s^{1.82}2p^{4.53}(3d^{0.03})$
ES1	−0.46	$1s^{0.22}2p^{0.19}(3d^{0.05})$
ES2	−0.35	$1s^{0.16}2p^{0.14}(3d^{0.06})$

duction band at Γ is of Γ_{1+} symmetry, and has mainly Pb $6p_z$ and Pb $6s$ character. The direct band gap at the zone center Γ is 3.23 eV.

From the band-structure calculations we deduce for α-PbO an indirect band gap of 1.82 eV, which is in good agreement with the experimental value for the indirect gap at 300 K of 1.95 eV.[31,32] and with values for the indirect band gap of about 2.0 eV deduced from exciton absorption and photoluminescence measurements at 4 K.[33–36] Our calculated value is somewhat higher than the value calculated by De Groot,[37] who found 1.71 eV for the indirect band gap using the same method. The difference is due to the choice of a different set of Wigner-Seitz radii for the atoms, which slightly affects the value of the band gap. The bottom of the conduction band is at M, and the top of the valence band is along the Γ-X direction. The calculated direct band gap is at M, with a value of 3.21 eV, in reasonable agreement with the experimental values at 300 K of 2.75 eV (Ref. 31) and 2.84 eV.[32]

C. Band structure of β-PbO

The first Brillouin zone of β-PbO is given in Fig. 3(b). The dispersion of the energy bands in β-PbO is shown in Fig. 6, the total and partial density of states is shown in Fig. 7. Because the primitive unit cell for the high-temperature form of PbO is twice as large as for α-PbO, the number of bands in β-PbO is also twice as large, namely 16 versus 8 bands in the valence band. The charges and atomic configurations are tabulated in Table

TABLE IV. Energy [with and without spin-orbit (SO) splitting], orbital character, and symmetry (without SO splitting) of the energy bands at Γ for α-PbO. The energy is given with respect to the state of the valence band with the highest energy at Γ, and the orbital character is in order of decreasing orbital contribution.

Energy (eV) With SO	Energy (eV) Without SO	Character	Symmetry
−6.99	−7.01	O $2p_z$, Pb $6s$	3^-
−6.10	−6.25	Pb $6s$	1^+
−4.65	−4.46	O $2p_{x,y}$	5^+
−4.42			
−2.16	−2.12	O $2p_z$	2^+
−1.96	−1.84	O $2p_{x,y}$	5^-
−1.87			
0.00	0.00	O $2p_z$, Pb $6s$	3^-
3.23	3.34	Pb $6p_z$, Pb $6s$	1^+

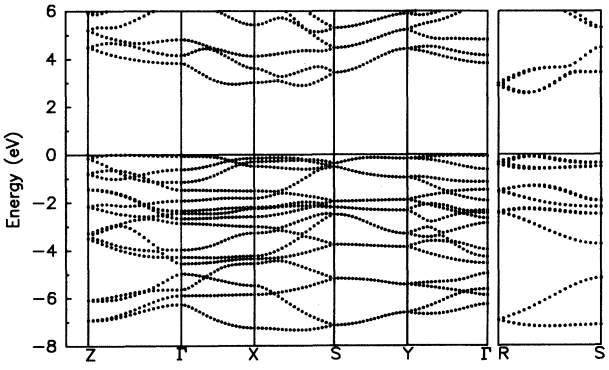

FIG. 6. The band structure of β-PbO; the energies are with respect to the top of the valence band.

V, the symmetry and wave function character of the valence-band states and the lowest conduction-band states are listed in Table VI. Only orbitals that contribute more than 10% are listed.

Contrary to α-PbO, the valence band consists of three clearly separate parts. The dispersion of the bands is quite small throughout the whole Brillouin zone. The bottom of the valence band is formed by four bands, the middle of the valence band contains eight bands, and the top of the valence band consists of four bands.

The bottom of the valence band has predominantly Pb $6s$ character, hybridized mainly with O $2p$ states (see Fig. 7). The middle eight bands consist mainly of O $2p$ states, with some mixing with Pb $6p$ states. In the upper part of the valence band there is again a large contribution of O $2p$ states, hybridized with Pb $6s$ and Pb $6p$ states. The states at the bottom of the valence band have mainly Pb $6s$, O $2p_x$, and O $2p_y$ character in Γ. The state of the valence band with the highest energy at Γ, and the state of the conduction band with the lowest energy at Γ, both have Γ_{3-} symmetry. The top of the valence band has mainly O $2p_x$ and Pb $6s$ character, and the bottom of the conduction band has mainly Pb $6p_y$, Pb $6d_{xy}$, O $2p_y$, and some Pb $6p_x$ character. The direct band gap at the zone center is 3.99 eV.

According to our calculations, β-PbO has an indirect

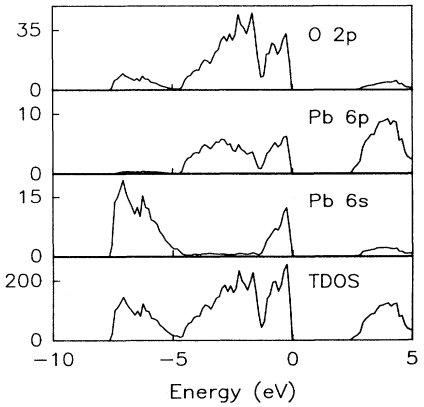

FIG. 7. Total and partial density of states for β-PbO.

TABLE V. Charges Q in the WS sphere and atomic configuration of atoms and empty spheres for β-PbO.

Atom	Q	Configuration
Pb	+1.46	$6s^{1.45}6p^{0.76}6d^{0.23}(5f^{0.10})$
O	−0.17	$2s^{1.77}2p^{4.37}(3d^{0.02})$
ES1	−0.66	$1s^{0.29}2p^{0.28}(3d^{0.09})$
ES2	−0.64	$1s^{0.25}2p^{0.27}(3d^{0.12})$

band gap of 2.57 eV. The top of the valence band is along the Γ-Z direction, the bottom of the conduction band is along the S-R direction. The calculated direct band gap lies at the position of the bottom of the conduction band and has a value of 2.66 eV. Experimentally an indirect band gap of about 2.7 eV at 300 K is observed.[31,32,38]

IV. X-RAY PHOTOEMISSION EXPERIMENTS ON PbO

A. Experiment

The samples used were obtained commercially from Aldrich (99.999% pure). Orthorhombic PbO was sintered in air at 880 K for three weeks.

The x-ray photoemission spectra were obtained using a small spot ESCA machine of Vacuum Generators with an Al $K\alpha$ x-ray source. The photon energy of the Al $K\alpha$ line is 1486.6 eV. Generally, a spot size of 300 μm or 600 μm was used. The resolution chosen was 0.2 eV.

At room temperature, charging of the nonconducting lead monoxides produced inconsistent results. To prevent charging, the spectra were taken at higher temperatures in order to increase the electrical conduction of the samples. The spectra of α-PbO were taken at approximately 400 K, and those of β-PbO at approximately 650 K. In order to clean the surfaces, the samples were scraped with a diamond scraper in a preparation chamber with a base pressure of 10^{-6} Pa. This was done very carefully, because mechanical treatment can induce the $\beta \rightarrow \alpha$ transition. The samples with fresh surfaces were transported to the main chamber (base pressure 10^{-8} Pa at room temperature) within half a minute.

TABLE VI. Energy (calculated with and without spin-orbit interaction), orbital character, and symmetry of the energy bands at Γ for β-PbO. The energy is given with respect to the state of the valence band with the highest energy at Γ, and the orbital character is in order of decreasing orbital contribution.

Energy (eV) With SO	Energy (eV) Without SO	Character	Symmetry
−6.21	−6.24	O $2p_x$, Pb $6s$	3^-
−5.85	−5.85	O $2p_y$, Pb $6s$	2^+
−5.53	−5.61	Pb $6s$	1^+
−4.92	−4.94	Pb $6s$, O $2p_x$, O $2p_y$	4^-
−4.51	−4.45	O $2p_z$, Pb $6p_z$	3^+
−4.24	−4.20	O $2p_y$, Pb $6p_y$	3^-
−3.95	−3.91	O $2p_x$	1^+
−2.83	−2.80	O $2p_z$	1^-
−2.64	−2.60	O $2p_z$	4^+
−2.41	−2.37	O $2p_y$	1^+
−2.31	−2.29	O $2p_x$	2^+
−1.88	−1.86	O $2p_x$, O $2p_y$	4^-
−1.45	−1.40	O $2p_z$	2^-
−1.07	−1.10	O $2p_y$, Pb $6s$	2^+
−0.56	−0.56	O $2p_y$, Pb $6s$, O $2p_x$	4^-
0.00	0.00	O $2p_x$, Pb $6s$	3^-
3.94	3.99	Pb $6p_y$	3^-
4.25	4.31	Pb $6p_x$	1^+

B. X-ray photoemission spectra

We measured x-ray photoemission spectra of some of the core levels of Pb, the O $1s$ line, and the valence band in both α-PbO and β-PbO. Before cleaning the surface, a wide scan spectrum between 0 and 1000 eV showed the presence of carbon on the sample. Also, a doublet structure is seen in the O $1s$ electron spectra, with a separation of 2 eV [Fig. 8(a)]. In earlier XPS studies on PbO, such a doublet structure for O $1s$ was always observed, and this was interpreted as evidence that both phases of PbO are present on the surface.[23,24] However, Thomas and Tricker[25] showed that the peak at high binding energy is due to contaminations. We also find that after cleaning no carbon contaminations are found on the surface, and for α-PbO the O $1s$ peak at the higher binding energy (BE) has nearly disappeared [Fig. 8(b)]. For β-PbO, only a single O $1s$ peak is observed, at nearly the same position as α-PbO [Fig. 8(c)]. These observations clearly show that the O $1s$ peak at high BE is due to (carbon)-oxygen containing contaminations.

The results of the core levels are shown in Table VII. The reported binding energies are with respect to the Fermi energy of the sample. The full width at half maximum (FWHM) of the peaks is between brackets. The core levels of α-PbO are at higher binding energy than in β-PbO. The width of the Pb $4f$ peaks is somewhat smaller than reported in the literature, but the spin-orbit splitting of 4.8–4.9 eV is the same.

The valence bands XPS of α-PbO and β-PbO are

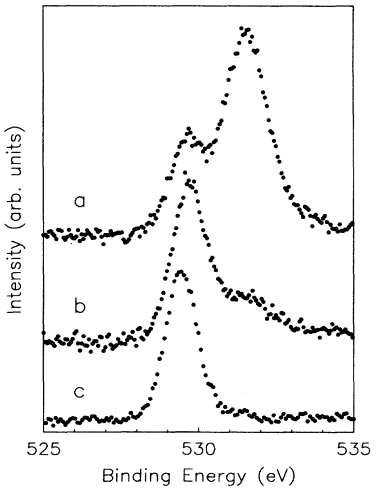

FIG. 8. X-ray photoelectron spectra of O $1s$ core levels (a) α-PbO before cleaning, (b) α-PbO after cleaning, (c) β-PbO after cleaning.

TABLE VII. Binding energy (eV) and width (FWHM) of core levels of α-PbO and β-PbO.

Peak	α-PbO	β-PbO
Pb $5d_{5/2}$	20.5 (1.3)	19.4 (1.3)
Pb $5d_{3/2}$	23.1 (1.3)	22.1 (1.3)
Pb $5p_{3/2}$	85.2 (6.2)	84.4 (6.0)
Pb $5p_{1/2}$	108.8 (5.9)	108.0 (6.0)
Pb $4f_{7/2}$	138.6 (1.4)	138.2 (1.2)
Pb $4f_{5/2}$	143.6 (1.4)	143.0 (1.2)
Pb $4d_{5/2}$	414.2 (4.0)	413.1 (4.2)
Pb $4d_{3/2}$	436.4 (4.0)	435.5 (4.2)
Pb $4p_{3/2}$	645.8 (5.1)	644.7 (4.6)
O 1s	529.7 (1.4)	529.4 (1.2)

shown in Fig. 9. The spectra of both α-PbO and β-PbO are very much alike, a consist of three peaks, one of which is clearly separated from the other two. In Fig. 9 we also give a calculated spectrum, obtained from the partial density of states (see Figs. 5 and 7) multiplied by the cross sections.[39] The calculated spectra agree quite well with the observed photoelectron spectra. The large intensity of the first peak below the top of the valence band is direct evidence of the large contribution of Pb 6s states to this band.

According to Fig. 9, the top of the valence band in α- and β-PbO lies below the Fermi level, at binding energies of 2.6 and 1.4 eV, respectively. The difference of 1.2 eV is of the same order as the difference between the binding energies of the core levels of α- and β-PbO (see Table VII). This indicates that the energies of the core levels with respect to the top of the valence band are approximately the same for α- and β-PbO.

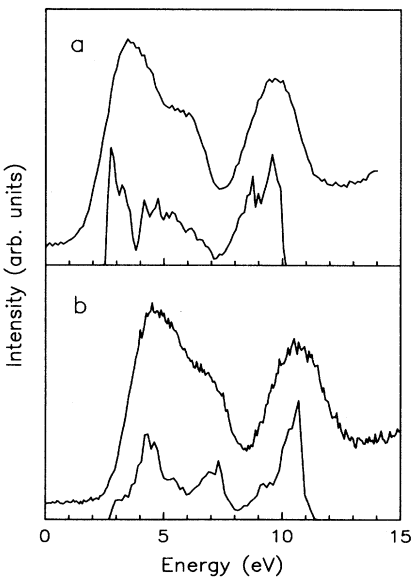

FIG. 9. Experimental (top) and calculated (bottom) valence band spectrum of (a) β-PbO, (b) α-PbO.

V. DISCUSSION OF THE BAND STRUCTURE OF PbO

In a previous section we have reported results of *ab initio* band-structure calculations of α- and β-PbO. The band structures show a band at a binding energy of about 8.6 eV, consisting mainly of Pb 6s states hybridized with O $2p_z$. This band has a large dispersion in the direction perpendicular to the layers (ΓZ for α-PbO, ΓX for β-PbO) and a small dispersion in the layers. This means that overlap between Pb 6s orbitals of adjacent layers is large.

The four energy bands between binding energies of about 6.8 and 1.6 eV (consisting mainly of O $2p_{x,y}$ hybridized with Pb $6p_{x,y}$ in α-PbO) have a small dispersion perpendicular to the layers, and large dispersion in the layers, as expected. These bands are mainly responsible for intralayer Pb-O bonding. The narrow band (width about 1.5–2 eV) at the top of the valence band is dominated by O $2p_z$ states, but it has also an appreciable contribution of Pb 6s and Pb $6p_z$ orbitals.

The calculated width of the valence band is somewhat different for the two PbO modifications; it is 8.6 eV for α-PbO and 7.8 eV for β-PbO. XPS spectra show hardly any difference between the widths for the valence bands of α- and β-PbO (Fig. 9). The values of the direct and indirect energy gaps of α- and β-PbO, obtained with the ASW method, agree quite well with the experimental values. Part of this agreement may well be fortuitous, in view of the uncertainty in the choice of the Wigner-Seitz radii. However, the fact that the band gaps agree with the observed values within 0.2–0.5 eV, is quite remarkable; in the classical semiconductors, like silicon and germanium, the calculated band gap is much smaller than the experimental value. We remark that for SnS,[40] which is a IV-VI semiconductor like PbO, and also for FeS_2,[41] the energy gaps calculated with the ASW method are also quite close to the experimental values. We have no explanation for this difference between PbO, SnS, and FeS_2 on one hand, and the classical semiconductors on the other hand.

We compare our results for PbO with calculations of the electronic structure reported in the literature. Dickens[42] discussed qualitatively the bonding in PbO in terms of the hybridization of Pb and O orbitals. The chemical bonding was partly attributed to hybrid orbitals of lead ($6d_{z^2} \pm 6p_z$) overlapping with orbitals of the oxygen atoms. However, according to our calculations the contribution of Pb 6d orbitals to the chemical bonding in PbO is very small (Tables III and V). Evarestov and Veryazov carried out semiempirical LUC-CNDO (large unit cell–complete neglect of differential overlap) calculations of the electronic structure of lead oxides.[20,43] The reported data for the total density of states differs strongly from our results. The calculations by Evarestov and Veryazov do not reproduce the minimum in the density of states of the valence band, seen in our calculations (Figs. 5 and 7), and also observed in the XPS valence band spectra (Fig. 9).

A detailed discussion of chemical bonding in α- and β-PbO, based on semiempirical extended Hückel tight-binding calculations, was presented by Trinquier and

Hoffmann.[19] The symmetry and orbital character of the bands at different points in the Brillouin zone obtained by these authors, is in general agreement with our results. However, the calculations by Trinquier and Hoffmann show a much larger dispersion of the upper valence band. According to these authors this band consists mainly of Pb 6*s* orbitals, and actually represents the lone pair of electrons on the lead atom. Our calculations show that the Pb 6*s* orbitals contribute mainly to the lowest valence band. The calculated total density of states reported by Trinquier and Hoffmann is not in agreement with the experimental XPS spectrum. Moreover, the calculations by Trinquier and Hoffmann lead to values for the energy gap of 4.96 eV for α-PbO and of 5.90 eV for β-PbO, values that are much larger than the observed values.

VI. THE "INERT" ELECTRON PAIR IN Pb(II)

B subgroup metal atoms such as Tl, Pb, Bi, Sn, and Sb, exhibit in many compounds a valency two smaller than the group valency. The sterochemistry of molecules and solids with ions of these unusual valencies is very complicated, in many cases the coordination of the metal atom is highly asymmetric. There is a recent revival of interest in this subject because several of the new high-T_c superconducting oxides contain ions of this type [Tl(I), Pb(II), Bi(III), etc.].

The free ions of the lower valency, i.e., Pb(II), Bi(III), all have, in addition to filled shells, a $(ns)^2$ electron configuration. Ions with this electronic configuration have a very large polarizability. Orgel[16] showed that the high polarizability of the lone pair can lead to a stabilization of a distorted coordination of Pb(II), Sn(II), Bi(III), and Tl(I) ions in ionic crystals. Indeed, PbO, SnO, and SnS are strongly distorted, whereas the more covalent compounds PbS, PbSe, PbTe, and SnTe have the NaCl structure, with the metal atoms in an undistorted octahedral coordination.

Le Bellac[44,45] has given a detailed discussion of the lone-pair effect in PbO in terms of the simple electrostatic model proposed by Orgel.[16] The calculated value of the dipole moment on Pb(II), obtained using the polarizability $\alpha(Pb^{2+})=4.9\times10^{-24}$ cm^3,[46] is very large: $\mu=9.6\times10^{-18}$ esu; it corresponds to a displacement of two electrons over a distance of 1 Å. The structural phase transitions $\alpha\rightarrow\beta$ and $\alpha\rightarrow\alpha'$ for PbO were explained by Le Bellac in terms of a change of the orientation of the lone pairs.

It is of interest to compare the distribution of Pb 6*s* states in α-PbO with that in cubic PbS.[47] In PbS there is also a narrow band at the bottom of the valence band. However, contrary to the situation in PbO, this band is nearly purely of Pb 6*s* character, with negligible hybridization with S 3*p* or Pb 6*p* orbitals. A consequence is that in PbS there is no band at the top of the valence band with a large contribution of Pb 6*s* states, as there is in PbO. Thus the so-called inert pair of electrons in PbS occupies the spherically symmetric Pb 6*s* states. This pair is not stereochemically active, it is indeed inert in PbS, in that it does not take part in the covalent bonding. In PbO the pair of electrons on Pb is much less inert. Its density of states is distributed over two bands, one at the top and one at the bottom of the valence band. The Pb 6*s* states are strongly hybridized with oxygen orbitals. This will make the charge distribution of electrons at lead highly asymmetric. The lead atoms in PbO are electrically polarized, with the lone pair sticking out at one side of the lead atom. Thus this pair of electrons in PbO is sterochemically active, and is responsible for the highly asymmetric coordination of the lead atoms in PbO.

ACKNOWLEDGMENTS

This work is part of the research program of the Stichting voor Scheikundig Onderzoek Nederland (SON), and is financially supported by the Nederlandse Organisatie voor Wetenschappelijk Onderzoek (NWO).

[1] J. Leciejewicz, Acta Crystallogr. **14**, 1304 (1961).
[2] J. Hill, Acta Crystallogr. Sec. C **41**, 1281 (1985).
[3] E. F. de Haan, A. van der Drift, and P. P. M. Schampers, Philips Tech. Rev. **25**, 133 (1967).
[4] J. R. Clark, A. K. Weiss, J. L. Donovan, J. E. Green, and R. E. King, J. Vac. Sci. Technol. **14**, 219 (1977).
[5] J. van den Broek, W. Kwestro, C. Langereis, and A. Netten, in *Proceedings of the Third International Conference on Photoconductivity,* edited by E. M. Pell (Pergamon, New York, 1971), p. 195.
[6] S. Radhakrishnan, M. N. Kamalasan, and P. C. Mehendra, J. Mater. Sci. **18**, 1912 (1983).
[7] P. C. Mehendru, S. Radhakrishnan, and M. Kamalasanan Conf. Rec. IAS Annu. Meet. (IEEE) **1980**, (2) 1153
[8] R. Clasen, J. Photogr. Sci. **28**, 226 (1980).
[9] J. Moreau, J. M. Kiat, P. Garnier, and G. Calvarin, Phys. Rev. B **39**, 10 296 (1989).
[10] A. Hédoux, D. Grebille, and P. Garnier, Phys. Rev. B **40**, 10 653 (1989).
[11] D. Le Bellac, J.-M. Kiat, A. Hédoux, P. Garnier, D. Grebille, Y. Guinet, and I. Noiret, Ferroelectrics **125**, 215 (1992).
[12] D. Grebille, P. Garnier, J. M. Kiat, and A. Hédoux, Phase Transitions **31**, 55 (1991).
[13] K. Chhor, C. Pommier, P. Garnier, and L. Abello, J. Phys. Chem. Solids **52**, 895 (1991).
[14] R. L. Withers and S. Schmid, J. Solid State Chem. **113**, 272 (1994).
[15] D. M. Adams, A. G. Christy, J. Haines, and S. M. Clark, Phys. Rev. B **46**, 11 358 (1992).
[16] L. E. Orgel, J. Chem. Soc. **1959**, 3815.
[17] K. S. Pitzer, Acc. Chem. Res. **12**, 271 (1979).
[18] P. Pyykkö and J. P. Desclaux, Acc. Chem. Res. **12**, 276 (1979).
[19] G. Trinquier and R. Hoffmann, J. Phys. Chem. **88**, 6696 (1984).
[20] R. A. Evarestov and V. A. Veryazov, Phys. Status Solidi B **165**, 401 (1991).
[21] G. A. Bordovskii, N. L. Gordeev, A. N. Ermoshkin, V. A. Izvozchikov, and R. A. Evarestov, Phys. Status Solidi B **111**, K123 (1982).
[22] G. A. Bordovskii, N. L. Gordeev, A. N. Ermoshkin, V. A. Iz-

vozchikov, and R. A. Evarestov, Phys. Status Solidi B **115**, K15 (1983).
[23]K. J. Kim, T. J. O'Leary, and N. Winograd, Anal. Chem. **45**, 2214 (1973).
[24]K. S. Kim and N. Winograd, Chem. Phys. Lett. **19**, 209 (1973).
[25]J. M. Thomas and M. J. Tricker, J. Chem. Soc. Faraday Trans. 2 **71**, 329 (1975).
[26]A. R. Williams, J. Kübler, and C. D. Gelatt, Jr., Phys. Rev. B **19**, 6094 (1979).
[27]U. von Barth and L. Hedin, J. Phys. C **5**, 1629 (1972).
[28]M. Methfessel and J. Kübler, J. Phys. F **12**, 141 (1982).
[29]K. S. Pitzer, Acc. Chem. Res. **12**, 271 (1979).
[30]*Tables of Irreducible Representations of Space Groups and Corepresentations of Magnetic Space Groups* (Pruett, Boulder, 1967).
[31]R. C. Keezer, D. L. Bowman, and J. H. Becker, J. Appl. Phys. **39**, 2062 (1968).
[32]J. van den Broek, Philips Res. Rep. **22**, 36 (1967).
[33]D. S. Nedzvetskii, V. A. Gaisin, N. Ya. Chistyakova, and M. K. Sheinkman, Fiz. Tekh. Poluprovodn. **14**, 1894 (1980) [Sov. Phys. Semicond. **14**, 1128 (1980)].
[34]V. A. Korneichuk, D. S. Nedzvetskii, N. Ya. Chistyakova, and M. K. Sheinkman, Fiz. Tverd. Tela (Leningrad) **21**, 2490 (1979) [Sov. Phys. Solid State **21**, 1436 (1979)].
[35]V. A. Gaisin, D. S. Nedzvetskii, V. I. Filipov, N. Ya. Chistyakova, and M. K. Sheinkman, Fiz. Tverd. Tela (Leningrad) **21**, 2513 (1979) [Sov. Phys. Solid State **21**, 1451 (1979)].
[36]V. A. Gaisin, D. S. Nedzvetskii, V. I. Filipov, N. Ya. Chistyakova, and M. K. Sheinkman, Opt. Spektrosk. **48**, 775 (1980) [Opt. Spectrosc. (USSR) **48**, 428 (1980)].
[37]R. A. de Groot, Physica (Amsterdam) **172B**, 45 (1991).
[38]K. Iinuma, T. Seki, and M. Wada, Mat. Res. Bull. **2**, 527 (1967).
[39]J. J. Yeh and I. Lindau, At. Data Nucl. Data Tables **32**, 1 (1985).
[40]A. R. H. F. Ettema, R. A. de Groot, C. Haas, and T. S. Turner, Phys. Rev. B **46**, 7363 (1992).
[41]W. Folkerts, G. A. Sawatzky, C. Haas, R. A. de Groot, and F. U. Hillebrecht, J. Phys. C **20**, 4135 (1987).
[42]B. Dickens, J. Inorg. Nucl. Chem. **27**, 1495 (1965).
[43]R. A. Evarestov and V. A. Veryazov, Phys. Status Solidi B **165**, 411 (1991).
[44]D. Le Bellac, dissertation, Paris, 1993.
[45]D. Le Bellac, J. M. Kiat, and P. Garnier, J. Solid State Chem. **114**, 459 (1995).
[46]J. R. Tessman, A. H. Kahn, and W. Shockley, Phys. Rev. **92**, 890 (1953).
[47]A. R. H. F. Ettema, C. Haas, P. Moriarty, and G. Hughes, Surf. Sci. **287/288**, 1106 (1993).